24th INTERNATIONAL CONGRESS ON SOUND AND VIBRATION
23–27 July 2017, London

A GENERAL THEORY FOR LAYERED THICK SHELL OF A MAGNETORHEOLOGICAL FLUID CORE

Shyh-Chin Huang

Ming Chi University of Technology, Mechanical Engineering, New Taipei City 24301, Taiwan
email: schuang@mail.mcut.edu.tw

Chao-Yang Tsai

Department of Mechanical Engineering, Army Academy ROC, Taoyuan, Taiwan,

Dynamic equations for layered (sandwich) thick shell with magnetorheological fluid (MRF) core were derived. The governing differential equations, after sequential simplifications, contain only five displacements, one transverse, two in-plane and two shear angles of the bottom layer (host). The theory is general and can be specialized for many commonly seen structures such as beams, plates, spherical and cylindrical shells. The theory can also degenerate into single or two-layer structures by letting one or two layers' thickness vanish without causing any equation singularity. The case of a cylindrical thick shell was particularly discussed with the parameters variation such as layers' thickness and core's magnetic intensity. Numerical results proved that MRF core is superior to passive VEM core in adjusting natural frequency and damping quantity. The results also revealed that the maximum loss factor usually occurred at the lowest modes. The natural frequencies increased with the magnetic field intensity and reached saturation, eventually. The loss factors, yet, increased with the magnetic intensity up to a maximum value and then dropped with further increase of magnetic intensity. The natural frequencies decrease with thicker MRF layer but increase with top layer thickness.
Keywords: Sandwich structure, magnetorheological fluid, damping treatment

1. Introduction

Sandwich structures are commonly seen in engineering applications. One of the most frequent one is the so-called constrained layer damping (CLD) treatment. It is a three-layer element with the bottom as the host and a viscoelastic material (VEM) layer in the middle. The top layer is usually a stiff metal, called constraining layer, to generate larger shear stress in VEM. CLD has been proven to be a very effective approach to reducing structure vibration and noise. Earlier works about sandwich beam with a viscoelastic material (VEM) core could be referred to Kerwin [1] and DiTaranto [2]. Mead and Markus [3] further extended their theories. Many researchers afterwards adopted those theories to study the damping mechanism of various applications. In summary, a very thin VEM layer is usually enough to generate significant damping but not to change the frequency. Johnson [4] summarized the published CLD treatments prior to 1995 and compared to other approaches. The damping capacity of CLD treatment, due to its passive nature, is not aseffective as some new techniques, e.g. PZT shunt damping, magnetorheological (MR) and electorheological (ER) treatment. ER and MR fluids technologies were discovered and developed about at the same years of 1940s. Rabinov discovered the MRF effect at the US National Bureau of Standards [5, 6]. Wislow worked on the ERF technology.

A sandwich structure with a MR/ER fluid as the core is a sort of semi-active structure, or called the smart/adaptive structure. The shear modulus and loss factor of the structure can be reversibly and rapidly controlled by an external magnetic field or electronic field. Yalcintas and Dai [7] com-

pared the vibration control capabilities of ER- and MR-cored beam and concluded that both of ER and MR can reduce the vibration up to 30% and increase the natural frequency even to 100%. They recommended use MR for higher frequency operation and ER for lower one. Sun et al. [8] investigated the dynamic response of a MR sandwich beam using energy approach and compared the results with the experimental results. Yeh [9] investigated the dynamic properties of a MR sandwich rectangular plates using FEM and concluded that the thickness of the MR fluid layer has a significant influence on the natural frequency and modal loss factor. Yeh [10] also illustrated the damping of orthotropic sandwich cylindrical shells with an ER fluid core using a discrete FEM. Mohammadi and Sedaghati [11] developed a nonlinear FEM for a cylindrical shell panel with an ER core and studied the parametric effect of thickness ratio and field intensity. They found the loss factor first increased with ER core thickness and decreased after a best thickness ratio. Mikhasev et al [12] adopted the equivalent single layer (ESL) models to investigate the effect of applied magnetic field on eigenmodes, natural frequencies and damping ratios of thin laminated cylindrical shell containing MRF.

The present research is based on the previous theory developed by Huang et al [13], the governing differential equations are in terms of host's five displacements: two in-plane, two rotations and one transverse. The general equations can be degenerated into sandwich beam and plate if the structure curvatures vanish. The vibration equations for a three-layer thick cylindrical shell with a magnetorheological fluid (MRF) core are demonstrated and numerical results of parametric effects are illustrated and are discussed in this paper.

2. Analytical formulation

Consider a sandwich element with a MRF core, as shows in Fig. 1(a). The two surface layers are assumed elastic, homogeneous and isotropic. $(\alpha_1,\alpha_2,\alpha_3)$ is a set of orthogonal, curvilinear coordinates, where α_1 and α_2 denote the in-plane coordinates attached to the middle surface of the host (bottom layer) and α_3 is the transverse coordinate. In the following, the symbols *E*, *G*, *h*, μ and ρ denote Young's modulus, shear modulus, thickness, Poisson's ratio, and density, respectively. A subscript *j=1, 2, 3* denotes the coordinate direction and a superscript *i=s, m, c* stands for shell (bottom), MRF (core), and cover layer (top), respectively. Apply the Love's assumption that displacements vary linearly through the whole thickness. The displacements of all layers, as shown in Fig. 1(b), can be expressed as

$$\begin{aligned}
&U_j^s(\alpha_1,\alpha_2,\alpha_3) = u_j^s(\alpha_1,\alpha_2) + \alpha_3\beta_j^s(\alpha_1,\alpha_2)\ ,\\
&U_j^m(\alpha_1,\alpha_2,\alpha_3) = u_j^m(\alpha_1,\alpha_2) + \left(\alpha_3 - \frac{h^s+h^m}{2}\right)\beta_j^m(\alpha_1,\alpha_2)\ ,\ j=1,2\\
&U_j^c(\alpha_1,\alpha_2,\alpha_3) = u_j^c(\alpha_1,\alpha_2) + \left(\alpha_3 - \frac{h^s+2h^m+h^c}{2}\right)\beta_j^c(\alpha_1,\alpha_2)\ ,\\
&U_3(\alpha_1,\alpha_2,\alpha_3) = u_3(\alpha_1,\alpha_2)
\end{aligned} \quad . \tag{1}$$

where *U*'s denote the 3-D displacement functions of all layers and *u*'s stand for their corresponding middle surface displacements. β*'s* are the layers' rotation angles. The MRF's deformation can be expressed by the two surface layers' as

$$\begin{aligned}
u_j^m &= \frac{1}{2}\left[\left(u_j^c - \frac{h^c}{2}\beta_j^c\right) + \left(u_j^s + \frac{h^s}{2}\beta_j^s\right)\right],\\
\beta_j^m &= \frac{1}{h^m}\left[\left(u_j^c - \frac{h^c}{2}\beta_j^c\right) - \left(u_j^s + \frac{h^s}{2}\beta_j^s\right)\right],\ j=1,2
\end{aligned} \quad . \tag{2}$$

where

$$\beta_j^i = \frac{1}{f_j^i}\left(\frac{\partial u_j^i}{R_j^i} - \frac{1}{A_j^i}\frac{\partial u_3}{\partial \alpha_j}\right),\ i = s,c,\ j = 1,2\,. \tag{3}$$

A's and *R's*, in the above expressions, are the Lame parameters and the radii of curvature.

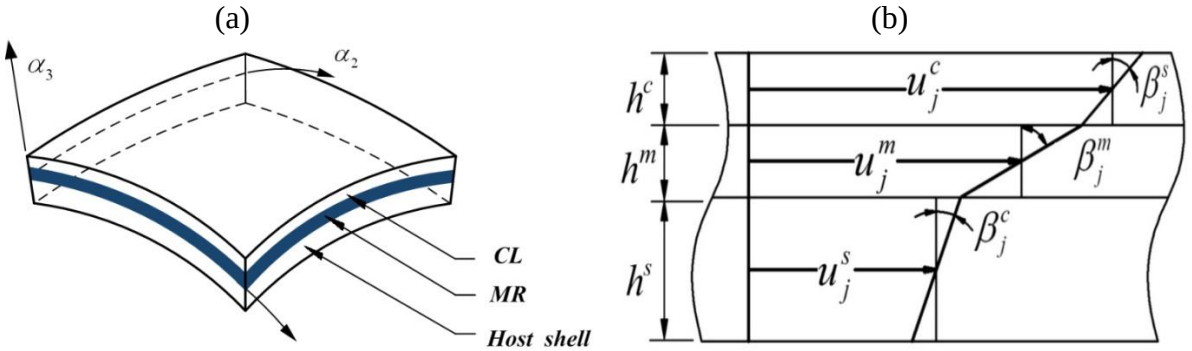

Figure 1**:** (a) Three-layer shell and its curvilinear coordinates and (b) displacement configuration.

3. Governing equations for a sandwich cylindrical shell

The authors have derived a theory for a three-layer, thick and general shell based on Hamilton's principle and Donnell-Mushtari-Vlaso assumptions [13]. The governing equations of the sandwich structure can be in terms of just the host's five displacement functions, u_1^s, u_2^s, u_3, β_1^s and β_2^s, as the following,

$$\begin{aligned}
&-\frac{\partial\left(N_{11}^s A_2^s\right)}{\partial\alpha_1} + N_{22}^s\frac{\partial A_2^s}{\partial\alpha_1} - \frac{\partial\left(N_{12}^s A_1^s\right)}{\partial\alpha_2} - N_{12}^s\frac{\partial A_1^s}{\partial\alpha_2} - k_s' G^s \varepsilon_{13}^s h^s \frac{A_1^s A_2^s}{R_1^s} \\
&-\left(\frac{2R_1^m + h^s + 2h^m}{2R_1^m + h^s}\right)\left[\frac{\partial\left(N_{11}^c A_2^c\right)}{\partial\alpha_1} - N_{22}^c\frac{\partial A_2^c}{\partial\alpha_1} + \frac{\partial\left(N_{12}^c A_1^c\right)}{\partial\alpha_2} + N_{12}^c\frac{\partial A_1^c}{\partial\alpha_2}\right] + \bar{m}^s\ddot{u}_1^s = 0
\end{aligned} \tag{4}$$

$$\begin{aligned}
&-\frac{\partial\left(N_{12}^s A_2^s\right)}{\partial\alpha_1} - N_{12}^s\frac{\partial A_2^s}{\partial\alpha_1} - \frac{\partial\left(N_{22}^s A_1^s\right)}{\partial\alpha_2} + N_{11}^s\frac{\partial A_1^s}{\partial\alpha_2} - k_s' G^s \varepsilon_{23}^s h^s \frac{A_1^s A_2^s}{R_2^s} \\
&-\left(\frac{2R_2^m + h^s + 2h^m}{2R_2^m + h^s}\right)\left[\frac{\partial\left(N_{12}^c A_2^c\right)}{\partial\alpha_1} N_{12}^c\frac{\partial A_2^c}{\partial\alpha_1} + \frac{\partial\left(N_{22}^c A_1^c\right)}{\partial\alpha_2} + -N_{11}^c\frac{\partial A_1^c}{\partial\alpha_2}\right] + \bar{m}^s\ddot{u}_2^s = 0
\end{aligned} \tag{5}$$

$$\begin{aligned}
&-\frac{\partial\left(M_{11}^s A_2^s\right)}{\partial\alpha_1} + M_{22}^s\frac{\partial A_2^s}{\partial\alpha_1} - \frac{\partial\left(M_{12}^s A_1^s\right)}{\partial\alpha_2} - M_{12}^s\frac{\partial A_1^s}{\partial\alpha_2} + k_s' G^s \varepsilon_{13}^s h^s f_1^s A_1^s A_2^s \\
&-\frac{h^s}{h^c}\left(\frac{2R_1^m + h^s + 2h^m}{2R_1^m + h^s}\right)\left[-\frac{\partial\left(M_{11}^c A_2^c\right)}{\partial\alpha_1} + M_{22}^c\frac{\partial A_2^c}{\partial\alpha_1} - \frac{\partial\left(M_{12}^c A_1^c\right)}{\partial\alpha_2} - M_{12}^c\frac{\partial A_1^c}{\partial\alpha_2}\right] + \bar{I}^s\ddot{\beta}_1^s = 0
\end{aligned} \tag{6}$$

$$\begin{aligned}
&-\frac{\partial\left(M_{12}^s A_2^s\right)}{\partial\alpha_1} - M_{12}^s\frac{\partial A_2^s}{\partial\alpha_1} + M_{11}^s\frac{\partial A_1^s}{\partial\alpha_2} - \frac{\partial\left(M_{22}^s A_1^s\right)}{\partial\alpha_2} + k_s' G^s \varepsilon_{23}^s h^s f_2^s A_1^s A_2^s \\
&-\frac{h^s}{h^c}\left(\frac{2R_2^m + h^s + 2h^m}{2R_2^m + h^s}\right)\left[-\frac{\partial\left(M_{12}^c A_2^c\right)}{\partial\alpha_1} - M_{12}^c\frac{\partial A_2^c}{\partial\alpha_1} - \frac{\partial\left(M_{22}^c A_1^c\right)}{\partial\alpha_2} + M_{11}^c\frac{\partial A_1^c}{\partial\alpha_2}\right] + \bar{I}^s\ddot{\beta}_2^s = 0
\end{aligned} \tag{7}$$

$$
\begin{aligned}
&-k_s' G^s h^s \frac{\partial\left(\varepsilon_{13}^s A_2^s\right)}{\partial \alpha_1} - k_s' G^s h^s \frac{\partial\left(\varepsilon_{23}^s A_1^s\right)}{\partial \alpha_2} + N_{11}^s \frac{A_1^s A_2^s}{R_1^s} + N_{22}^s \frac{A_1^s A_2^s}{R_2^s} + N_{11}^c \frac{A_1^c A_2^c}{R_1^c} + N_{22}^c \frac{A_1^c A_2^c}{R_2^c} \\
&-\frac{\partial}{\partial \alpha_1}\left\{\frac{1}{A_1^m}\left(\frac{2R_1^m h^m}{2R_1^m + h^s}\right)\left[\frac{\partial\left(N_{11}^c A_2^c\right)}{\partial \alpha_1} - N_{22}^c \frac{\partial A_2^c}{\partial \alpha_1} + \frac{\partial\left(N_{12}^c A_1^c\right)}{\partial \alpha_2} + N_{12}^c \frac{\partial A_1^c}{\partial \alpha_2}\right]\right\} \\
&-\frac{\partial}{\partial \alpha_2}\left\{\frac{1}{A_2^m}\left(\frac{2R_2^m h^m}{2R_2^m + h^s}\right)\left[\frac{\partial\left(N_{12}^c A_2^c\right)}{\partial \alpha_1} + N_{12}^c \frac{\partial A_2^c}{\partial \alpha_1} + \frac{\partial\left(N_{22}^c A_1^c\right)}{\partial \alpha_2} - N_{11}^c \frac{\partial A_1^c}{\partial \alpha_2}\right]\right\} + \bar{m}\ddot{u}_3 = 0
\end{aligned}
\quad . \tag{8}
$$

where all the parameters can be referred to reference [13].

The general three-layer thick shell equations are now specialized for a cylindrical shell in this study. The curvatures *R*'s and Lame *A*'s parameters of a cylindrical shell are constants and their derivatives will vanish. Let a^s, a^m and a^c denote the three layers' radii and $\alpha_1 = x$, $\alpha_2 = \theta$, $\alpha_3 = z$, Eqs. (4-8) become

$$
-a^s \frac{\partial N_{xx}^s}{\partial x} - \frac{\partial N_{x\theta}^s}{\partial \theta} - a^c \frac{\partial N_{xx}^c}{\partial x} - \frac{\partial N_{x\theta}^c}{\partial \theta} + \bar{m}^s \ddot{u}_x^s = 0 \,, . \tag{9}
$$

$$
-a^s \frac{\partial N_{x\theta}^s}{\partial x} - \frac{\partial N_{\theta\theta}^s}{\partial \theta} - k_s' G^s \varepsilon_{\theta z}^s h^s - \frac{2a^m + h^s + 2h^m}{2a^m + h^s}\left(a^c \frac{\partial N_{x\theta}^c}{\partial x} + \frac{\partial N_{\theta\theta}^c}{\partial \theta}\right) + \bar{m}^s \ddot{u}_\theta^s = 0 \,, . \tag{10}
$$

$$
\begin{aligned}
&N_{\theta\theta}^s + N_{\theta\theta}^c - k_s' G^s h^s a^s \frac{\partial \varepsilon_{xz}^s}{\partial x} - k_s' G^s h^s \frac{\partial \varepsilon_{\theta z}^s}{\partial \theta} - h^m\left(a^c \frac{\partial^2 N_{xx}^c}{\partial x^2} + \frac{\partial^2 N_{x\theta}^c}{\partial x \partial \theta}\right) \\
&-\frac{2h^m}{2a^m + h^s}\left(a^c \frac{\partial^2 N_{x\theta}^c}{\partial x \partial \theta} + \frac{\partial^2 N_{\theta\theta}^c}{\partial \theta^2}\right) + \bar{m}\ddot{u}_z = 0 \,,
\end{aligned}
\quad . \tag{11}
$$

$$
-\frac{\partial M_{x\theta}^s}{\partial \theta} - a^s \frac{\partial M_{xx}^s}{\partial x} + k_s' G^s \varepsilon_{xz}^s h^s a^s + \frac{h^s}{h^c}\left(a^c \frac{\partial M_{xx}^c}{\partial x} + \frac{\partial M_{x\theta}^c}{\partial \theta}\right) + \bar{I}^s \ddot{\beta}_x^s = 0 \,, . \tag{12}
$$

$$
-a^s \frac{\partial M_{x\theta}^s}{\partial x} - \frac{\partial M_{\theta\theta}^s}{\partial \theta} + k_s' G^s \varepsilon_{\theta z}^s h^s a^s + \frac{h^s}{h^c}\frac{2a^m + h^s + 2h^m}{2a^m + h^s}\left(a^c \frac{\partial M_{x\theta}^c}{\partial x} + \frac{\partial M_{\theta\theta}^c}{\partial \theta}\right) + \bar{I}^s \ddot{\beta}_\theta^s = 0 \,, . \tag{13}
$$

The shear modulus of the MRF was assumed complex as commonly seen and is adopted from Rajamohan et al. [14, 15] as

$$
G^m(G) = G'(G) + iG''(G) \,, . \tag{14}
$$

The real and imaginary parts of the modulus are commonly called the storage and the loss modulus, respectively. The storage modulus is a measure of MRF stiffness and the loss modulus determines how much energy is dissipated. Both the storage and loss modulus can be empirically expressed as functions of the intensity of magnetic field.

$$
\begin{aligned}
G'(G) &= -3.3691G^2 + 4997.5G + 873000 \,, \\
G'(G) &= -0.9G^2 + 812.4G + 185500,
\end{aligned}
\quad . \tag{15}
$$

where G is the intensity of magnetic of field in Gauss. The MRF core layer is assumed to be of VEM type embedded with magnetic particles. Hence, the characteristic of MRF is that its shear modulus can be changed by the external magnetic field. By the use of assumed mode method, choose a set of mode shapes which satisfy all of the boundary conditions and substitute it into the

corresponding EOMs. The complex eigenvalue for each (*m*,*n*) mode can be solved and the natural frequency ω_{mn} and loss factor η_{mn} are derived as

$$\lambda_{mn}^2 = \omega_{mn}^2(1+i\eta_{mn}),\ \omega_{mn}^2 = \mathrm{Re}(\lambda_{mn}^2), \eta_{mn} = \frac{\mathrm{Im}(\lambda_{mn}^2)}{\mathrm{Re}(\lambda_{mn}^2)}. \tag{16}$$

4. Numerical results and discussion

Numerical examples of a three-layer cylindrical shell with a MRF core are illustrated. The geometric and material properties for the numerical examples are, unless specified otherwise, given in Table 1. The five displacements of the host shell can be expressed as

$$\begin{cases} u_x(x,\theta,t) = A\cos\dfrac{m\pi x}{L}\cos n(\theta-\phi)e^{\lambda t} \\ u_\theta(x,\theta,t) = B\sin\dfrac{m\pi x}{L}\sin n(\theta-\phi)e^{\lambda t} \\ u_z(x,\theta,t) = C\sin\dfrac{m\pi x}{L}\cos n(\theta-\phi)e^{\lambda t} \end{cases}, \begin{cases} \beta_x(x,\theta,t) = F\cos\dfrac{m\pi x}{L}\cos n(\theta-\phi)e^{\lambda t} \\ \beta_\theta(x,\theta,t) = G\sin\dfrac{m\pi x}{L}\sin n(\theta-\phi)e^{\lambda t} \end{cases}. \tag{17}$$

where *m*, the axial wave number; *n*, the circumferential wave number; ϕ, an arbitrary phase angle; λ, the eigenvalue. Substituting Eq. (17) into Eqs. (9-13), it is obtained

$$\begin{bmatrix} a_{11}+\rho^s h^s\lambda^2 & a_{12} & a_{13} & a_{14} & a_{15} \\ a_{21} & a_{22}+\rho^s h^s\lambda^2 & a_{23} & a_{24} & a_{25} \\ a_{31} & a_{32} & a_{33}+\left(\dfrac{\rho^s h^s+\rho^m h^m a^m+\rho^c h^c a^c}{a^s}\right)\lambda^2 & a_{34} & a_{35} \\ 0 & 0 & a_{43} & a_{44}+\dfrac{\rho^s h^{s^3}}{12}\lambda^2 & a_{45} \\ 0 & a_{52} & a_{53} & a_{54} & a_{55}+\dfrac{\rho^s h^{s^3}}{12}\lambda^2 \end{bmatrix} \begin{Bmatrix} A \\ B \\ C \\ F \\ G \end{Bmatrix} = 0 \tag{18}$$

where all the coefficients a_{ij} are given in [13]. The determinant of Eq. (18) vanishes to yield the frequency equation of a three-layer cylindrical thick shell.

Figure 2 shows the natural frequencies and loss factors of m =1~6、n =0~20. The shell's first three natural frequencies correspond to (*m*,*n*)=(1,4), (1,5) and (1,3).

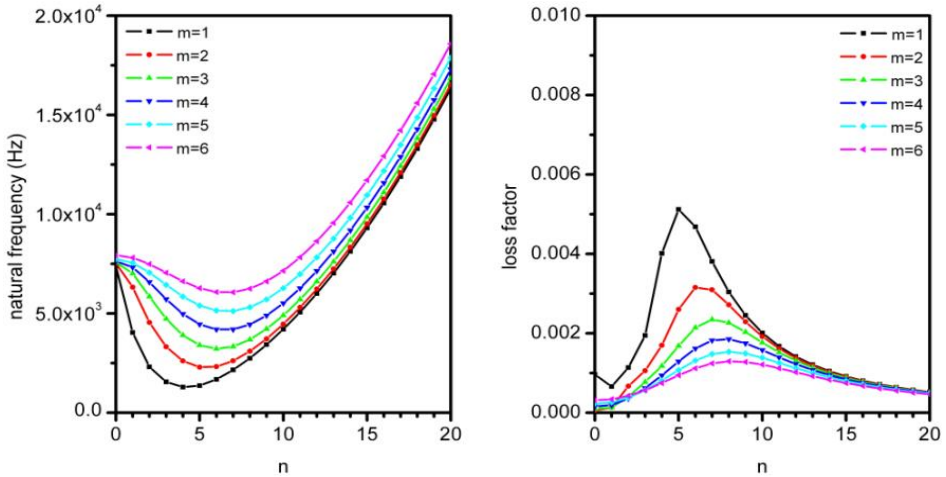

Figure 2: Natural frequencies and loss factors of the three-layer thick shell modes

Figure 3 illustrates the first four modes varying with G intensity. It is seen the natural frequency curves increase slowly with G and eventually go to flat (saturated) around G=800 but the loss factors increase with G sharply at the beginning and reach maxima. After that, further increase of G results in loss factors decrease for all modes. It means there is a best magnetic intensity for every mode as far as the loss factor is of concern. The present results show that the best G happens in the region of [300, 400]. One interesting observation is that the largest loss factor magnitude does not appear in the first mode.

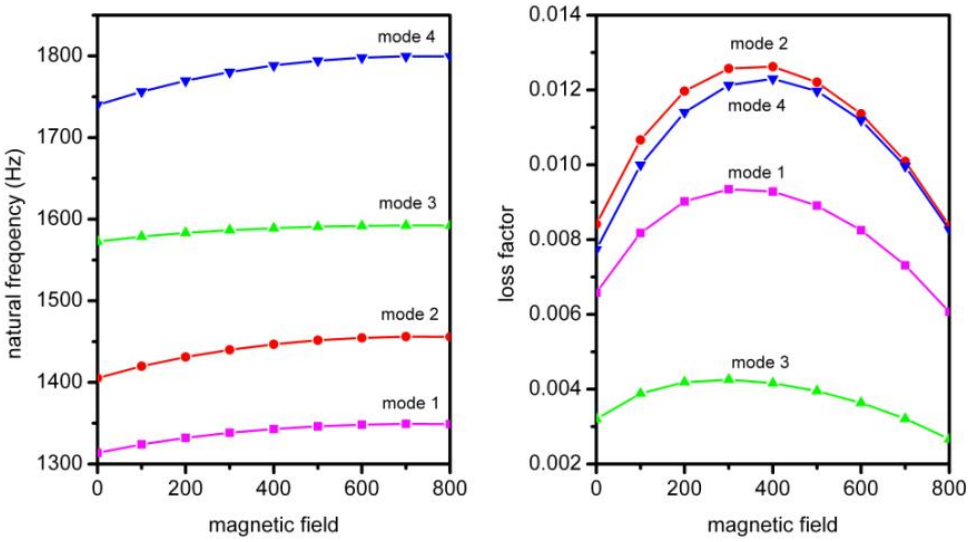

Figure 3: Natural frequency and loss factor varying with magnetic fields.

The effects of MRF layer thickness on the natural frequencies and the loss factor at G=400 are shown in Fig. 4. h_m^* is MRF thickness normalized with respect to the shell thickness. It is seen that the natural frequencies decrease with increasing MRF thickness and the decreasing rate at the higher modes is larger than that of the lower ones. As MRF thickness increases up to certain values there even exists mode exchange phenomenon. For instance, at $h_m^* = 0.5$, modes 3 and 4 exchange (dotted circle) and at $h_m^* = 0.7$, modes 1 and 2 exchange. The loss factors sharply decrease with MRF thickness at the beginning then become smoother afterward. The results infer that thicker MRF layer has no advantage as long as modal loss factor is the issue. Table 2 shows the values and improved percentage (in parentheses) of the first mode loss factor at various MRF thickness.

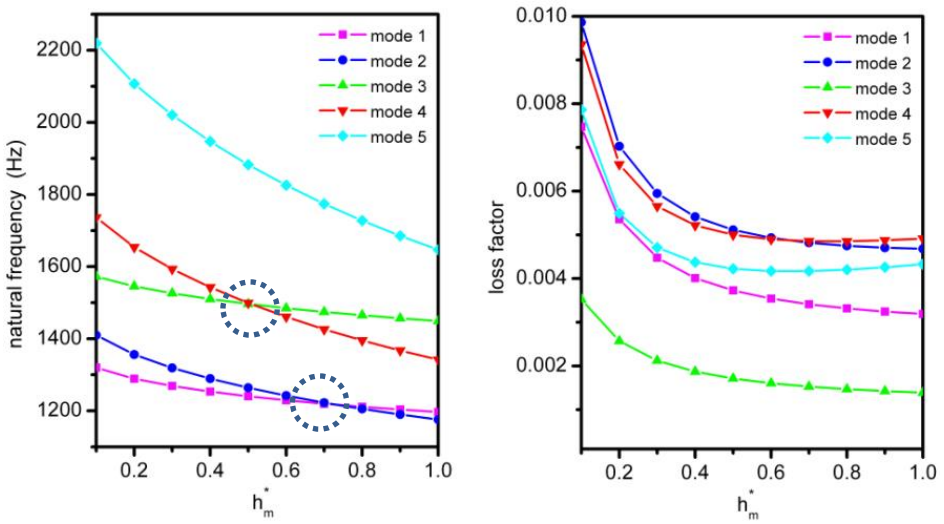

Figure 4**:** Natural frequencies and loss factors vary with MR's thickness h_m^*

Table 1**:** The geometric and material properties of the illustrated shell.

Host layer (Al)	L = 250 mm， a^s = 100 mm， h^s =2 mm， ρ^s = 2710 Kg/m^3， E^s = 70 GPa， μ^s = 0.3， k_s' =2/3
MRF	$G^m = G' + G''$， h^m = 0.254 mm， ρ^m = 3500 kg/m^3， k_v' =2/3
CL (Al)	h^c = 0.38 mm， ρ^c = 2710 kg/m^3， E^c = 70 GPa， μ^c = 0.3， k_c' =2/3

Table 2: Modal loss factors vary with magnetic field for different MRF's thickness for the first mode.

	Magnetic field		(m,n) =(1,4) (first mode)	
G	h_m^* **=0.12**	**0.14**	**0.16**	**0.18**
0	0.0042	0.0038	0.0035	0.0032
100	0.0055 (31.0%)	0.0050 (32.0%)	0.0046 (32.8%)	0.0043 (33.4%)
200	0.0063 (50.8%)	0.0058 (53.0%)	0.0054 (54.7%)	0.0050 (56.0%)
300	0.0067 (61.5%)	0.0062 (64.8%)	0.0058 (67.3%)	0.0055 (69.3%)
400	0.0069 (64.6%)	0.0064 (68.6%)	0.0060 (71.7%)	0.0056 (74.2%)
500	0.0067 (60.8%)	0.0062 (65.2%)	0.0059 (68.6%)	0.0055 (71.4%)
600	0.0063 (50.7%)	0.0059 (55.1%)	0.0055 (58.6%)	0.0052 (61.3%)
700	0.0056 (34.2%)	0.0052 (38.3%)	0.0049 (41.5%)	0.0047 (44.0%)

Figure 5 shows the case of varying top layer thickness from 0.1 to 0.3 for the first mode. It is seen that the natural frequencies increase with top layer's thickness but decreases with MRF's thickness. This is understandable because the top layer is metal and strengthens the whole structure as thickness increases. The MRF layer is formed of VEM matrix and softens the structure if thicker. The loss factors, however, decrease with both of the top layer's and MRF's thickness.

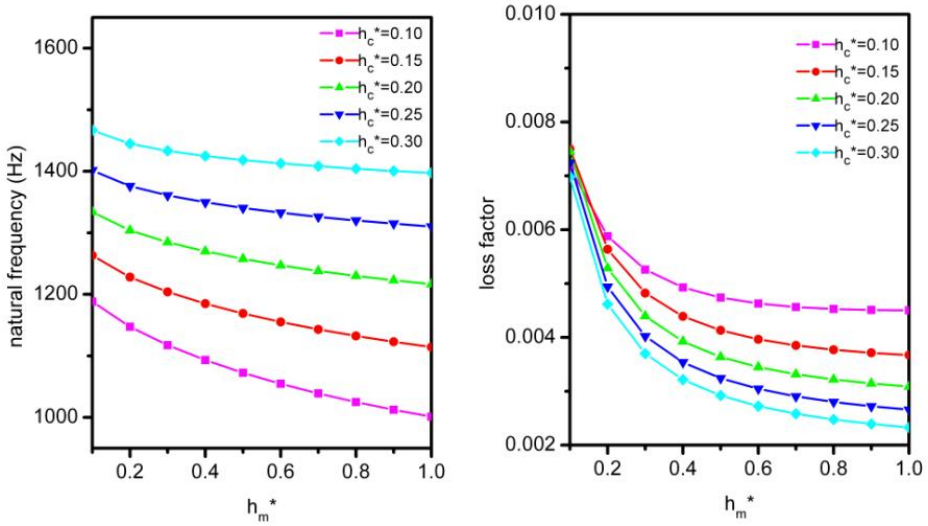

Figure 5: Natural frequency and loss factor vary with CL's thickness h_c^* of the first mode at G=400.

5. Conclusions

A general theory for thick sandwich shell with a MRF core was derived. Numerical studies were presented for a cylindrical shell. The results showed that the natural frequencies increase with mag-

netic field intensity but will reach saturation eventually. The modal loss factors significantly increase compared to no magnetic field, i.e., equivalent to a VEM layer. The improvement could be up to 70% for the first mode. The magnetic intensity was yet observed to have a best value for each mode and as it exceeds the best value the loss factor drops afterwards. The best G's were seen around 300 to 400 Gauss for the illustrated case. The effects of layers' thickness were studied as well. It was seen thicker MRF gains no advantage. The top layer's thickness increases the natural frequencies but not the modal loss factors.

Acknowledgement

The authors are grateful to Taiwan's Ministry of Science and Technology for the support of this research under the Grant No. MOST 105-2632-E-131-003.

REFERENCES

1. Kerwin, EM Jr. Damping of flexural waves by a constrained visco-elastic layer. *J Acoust Soc Am* 1959; 31: 952-962.
2. DiTaranto, RA. Theory of vibratory bending for elastic and viscoelastic layered finite length beams. *ASME J Appl Mech* 1965; 32: 881-886.
3. Mead, DJ and Markus, S. The forced vibration of a sandwich damping sandwich beam with arbitrary boundary conditions. *AIAA J* 1969; 10: 163-175.
4. Johnson, CD. Design of passive damping systems. *ASME* 1995; 117(special 50th anniversary design issue): 171-176.
5. Rabinow, J. The magnetic fluid clutch. *AIEE Transactions* 1948; 67: 1308-1315.
6. Rabinow, J. Magnetic fluid torque and force transmitting device. *U.S. PATENT* 1951; 2575360.
7. Yalcintas M and Dai H. Magnetorheological and electrorheological materials in adaptive structures and their performance comparison. *J Smart Mater Struct* 1999; 8: 560-573.
8. Sun, Q, Zhou, JX and Zhang, L. An adaptive beam model and dynamic characteristics of magnetorheological materials. *J Sound Vibr* 2003; 261(3): 465-481.
9. Yeh, JY. Vibration analysis of sandwich rectangular plates with magnetorheological fluid damping treatment. *Smart Mater Struct* 2013; 22: 035010.
10. Yeh, JY. Vibration and damping analysis of orthotropic cylindrical shells with electrorheological core layer. *Aerosp Sci Technol* 2011; 15: 293–303.
11. Mohammadi F and Sedaghati R. Nonlinear free vibration analysis of sandwich shell structures with a constrained electrorheological fluid layer. *Smart Mater Struct* 2012; 22: 075035.
12. Mikhasev, GI, Altenbach, H and Korchevskaya, EA. On the influence of the magnetic field on the eigenmodes of thin laminated cylindrical shells containing magnetorheological fluid. *Comput Struct* 2014; 113: 186-196.
13. Huang, SC, Liou, CL and Tsai, CY. A general vibration theory for constrained layer damping-treated thick sandwich structures. *J Sandwich Struct Mater* 2016; 18(3): 343-373.
14. Rajamohan, V, Rakheja, S and Sedaghati, R. Vibration analysis of a partially treated multi-layer beam with magnetorheological fluid. *J Sound Vibr* 2010; 329: 3451-69.
15. Rajamohan, V, Sedaghati, R and Rakheja, S. Optimum design of a multilayer beam partially treated with magnetorheological fluid. *J Smart Mater Struct* 2010; 19: 065002.